Fermi National Accelerator Laboratory

FERMILAB-Conf-97/392

Visible Light Photon Counters (VLPCs) for High Rate Tracking Medical Imaging and Particle Astrophysics

Muzaffer Atac

Fermi National Accelerator Laboratory
P.O. Box 500, Batavia, Illinois 60510

February 1998

Published Proceedings of the *7th ICFA School on Instrumentation in Elementary Particle Physics*, Leon, Guanajuato, Mexico, July 7-19, 1997

Operated by Universities Research Association Inc. under Contract No. DE-AC02-76CH03000 with the United States Department of Energy

Disclaimer

Distribution

Visible Light Photon Counters (VLPCs) for High Rate Tracking Medical Imaging and Particle Astrophysics

Muzaffer Atac

Fermi National Accelerator Laboratory
Batavia, IL 60510, U.S.A.
University of California at Los Angeles
Los Angeles, CA 90024, U.S.A.

Abstract. This paper is on the operation principles of the Visible Light Photon Counters (VLPCs), application to high luminosity-high multiplicity tracking for High Energy Charged Particle Physics, and application to Medical Imaging and Particle Astrophysics. The VLPCs as Solid State Photomultipliers (SSPMs) with high quantum efficiency can detect down to single photons very efficiently with excellent time resolution and high avalanche gains.

INTRODUCTION

High Energy Particle Physics experiments designed to run at high luminosity and high multiplicities require fine granularity, fast, good time resolution and good spatial resolution tracking. Scintillating fibers with the VLPC readout fulfill all these requirements. Scintillating fibers with a diameter less than 1mm can provide good multitrack resolution and high speed. The VLPCs with quantum efficiency around 80%, avalanche gain around 30,000, excellent time resolution (about 1nsec), and surface area of 1mm in diameter can provide an efficient tracking for High Energy Particle Physics (1) (2) (3). The VLPCs were developed by Rockwell International Science Center (now part of Boeing Co.) jointly with M. Atac, originally for UCLA under DOE contracts. The author has pioneered the development in 1987-88 under the contract for developing scintillating fiber tracking for High Energy Particle Physics, working together with Rockwell International Science Center, Anaheim, California. We called this research and development High Intensity Scintillating-fiber Tracking

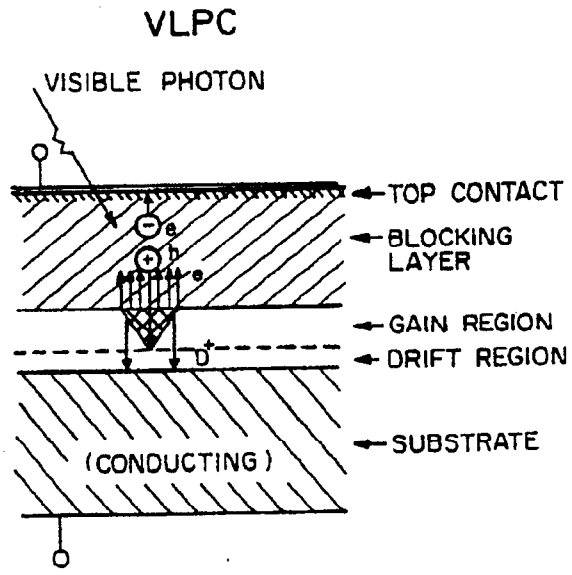

FIGURE 1. Schematic of the operational principles of the VLPC.

Experiment (HISTE) program. During the last few years the VLPCs have been purchased by E835 and D0 experiments at Fermilab. Fermilab physicists and engineers have been developing large systems for D0. 100,000 pixel VLPC system is needed for D0. E835 has done an experiment at Fermilab using a fiber tracker with a modest number of VLPCs (about 1200 channels). COSMOS (E803) collaboration has decided to put together a scintillating fiber tracking system with 40,000 fibers and VPLCs.

In the following we will also talk about application of VLPCs to Medical Imaging and Particle Astrophysics.

Before the VLPCs became practical in using for fiber tracking, UA2 Experiment used image intensifier readout with vacuum photocathode (4). This resulted in an inefficient tracking. Most image intensifier tubes are rather sensitive to magnetic fields. Tests done with the VLPCs showed no effect up to 12kG field.

OPERATING PRINCIPLES OF THE VLPCS

The operating principles of the VLPCs are given in Reference 2, therefore we will discussed them briefly here. The VLPCs are Impurity Band Conduction (IBC) devices that are minimized in quantum efficiency in the Infrared (IR) region while maximized in quantum efficiency for the wavelengths around 550nm relative to the original device, Solid State Photo Multiplier (SSPM), which was discovered by Rockwell International Science Center (5). The VLPCs are silicon based devices with some level of donor and acceptor concentrations in silicon formed by molecular epitaxy technique.

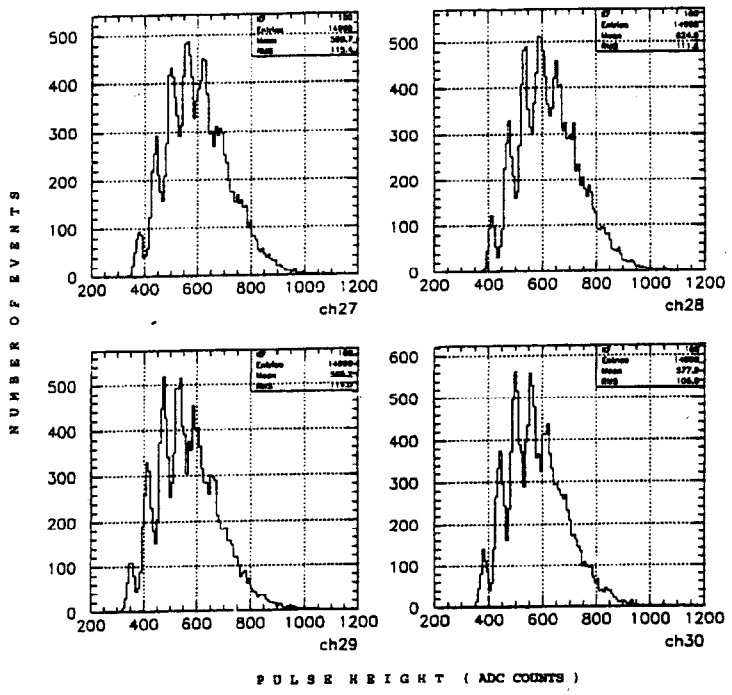

FIGURE 2. Multiple photoelectron peaks resulted when the VLPCs were illuminated with a pulsed LED. It shows uniform responses in quantum efficiency and gain from different channels obtainable under the same bias voltage.

A schematic diagram of the VLPC is shown in Figure 1. In a VLPC, a neutral donor is a substitutional ion with an electron bound to it in a hydrogen-like orbit with an ionization potential of about 0.05eV. Because of this very small energy gap, the devices need to run at cryogenic temperatures. Nominally they run at a temperature between 6 and 7K. When the concentration of impurities is sufficiently high, they form an energy band separated from the conduction band by the ionization potential. When the applied electric field is sufficiently high, about 2×10^3-10^4V/cm, each initial electron starts an avalanche of free electron-hole pairs within 1ns. The avalanche size could reach up to 5×10^4 when applied voltage reaches −7 volts. The avalanche may occupy about 10 micron diameter area for about few microseconds while the rest of the area is continuously available for detecting photons. The gain and the quantum efficiency (QE) of the devices taken from same wafer are very uniform at a common voltage and temperature as seen in Figure 2 (6). For this, photons from an LED illuminated the top of a cassette which housed the VLPCs. The photons then transmitted through optical fibers illuminating the VLPCs. The sensitive area of the devices was 1mm in diameter. They run in a space charge saturated avalanche mode. Due to the small gain dispersion, as seen in the figure, multi photoelectron peaks are

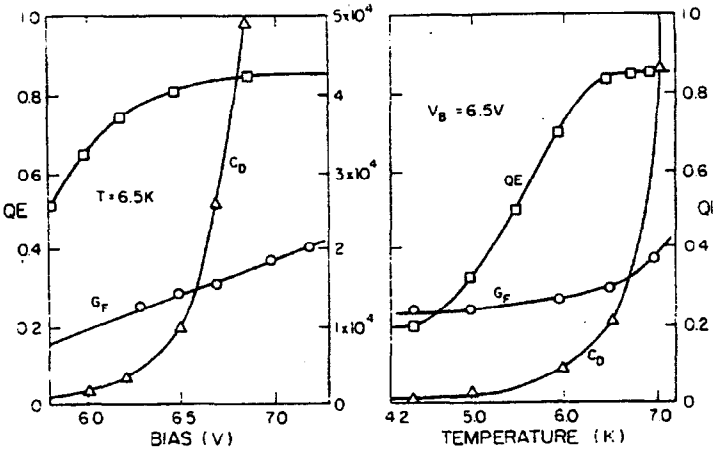

FIGURE 3. Quantum efficiency (QE) at A=560nm of an AR coated VLPC as functions of bias voltage and temperature is shown. Dark count pulse rate (C_D) and fast gain (G_F) are also indicated.

nicely separated. Due to their capability of counting photons, we called them Visible Light Photon Counters (VLPCs).

Because the devices are impurity semiconductors and the VLPC with arsenic impurity, that has a bandgap around 50 millielectron volt, it has to be operated at cryogenic temperatures, otherwise dark pulse (thermal electron pulse) rate would be extremely high (saturating the device). Figure 3 shows the quantum efficiency, the fast avalanche gain and dark pulse rate as functions of temperature and bias voltage. Optimum operating temperature is around 6.5K and optimum bias voltage is about 6.5V. The devices were coated with 560nm antireflective (AR) coating to improve the quantum efficiency (QE) from 70% to 85%. Operating the devices at 6.5K, controlling and monitoring the temperature within 0.1K are relatively easy.

Main characteristics of the VLPCs are summarized in the following table:

Table I.

Quantum efficiency optimized for 530nm	80%
Avalanche gain	$3\text{-}5\times10^4$
Thermal electron pulse rate at 6.5K	$\sim5\times10^3$/sec.mm
Saturation pulse rate	5×10^7/sec.mm
Pulse risetime	<3nsec
Average power per pixel	1.5 microwatt
Optimum operating voltage	~6.5V
Optimum operating temperature	6-7K
Dynamic range (linear)	3000 photoelectrons
Effect by magnetic field	no effect up to 12kG

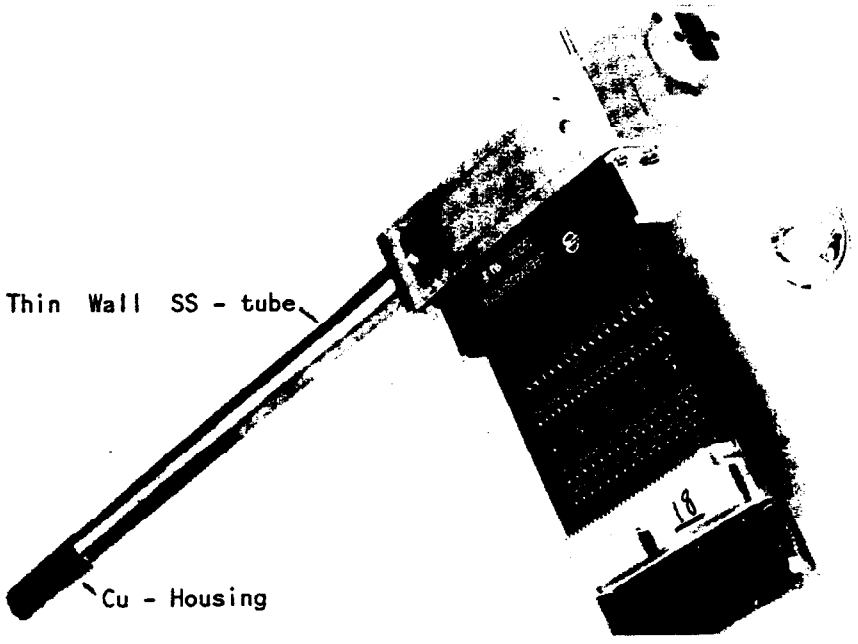

FIGURE 4. A photograph of a 32 channel VLPC cassette. The penny in the picture shows the compactness of the unit.

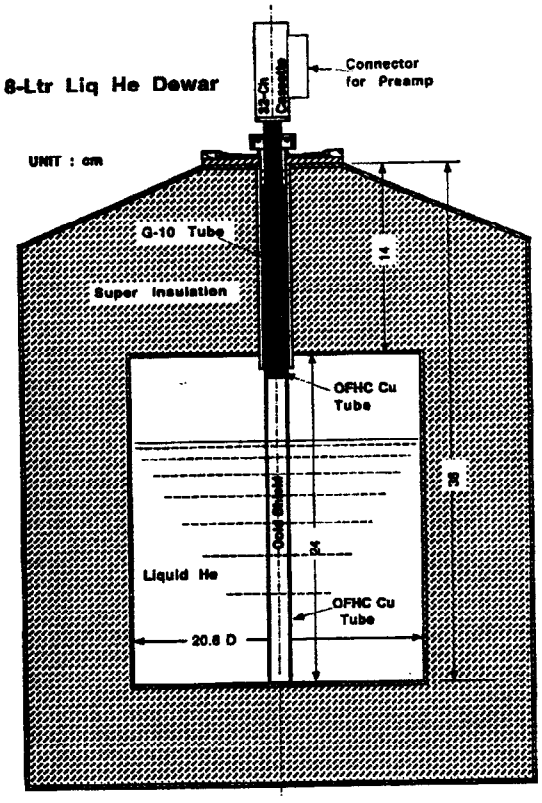

FIGURE 5. The structure of the 8-liter cryostat..

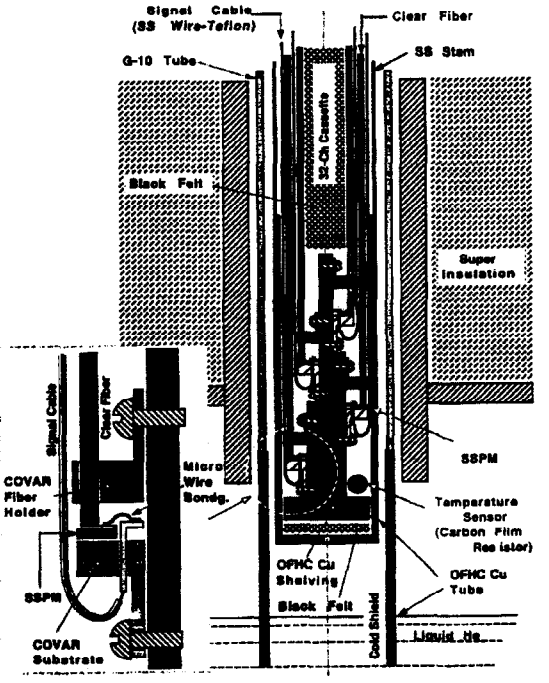

FIGURE 6. Enlarged view of the cassette.

PROTOTYPE CRYOGENIC CASSETTE DESIGN

A 32 channel VLPC cassette was designed by the author and constructed to carry out scintillating fiber tests for determining photoelectron yield from a variety of fibers, attenuation length of the photons in the fibers, and timing and rate capabilities of the VLPCs. Figure 4 shows one of the cassettes with a penny next to it. The penny is there to show how small a cryogenic system is used. At the top of the cassette a 32 channel of a QPAO2 amplifier is shown (7). The unit is designed to pass a small amount (about 50cc) of boil off liquid Helium (He) when inserted into a liquid He dewar. Details of the cassette-dewar assembly are shown in Figure 5. With the help of the Oxygen free High Conductivity Copper (OFHC) cold shield tubing, liquid He temperature is brought to the level of the OFHC housing in which the VLPCs are kept. With this arrangement the required temperature is reached and kept fairly constant over several days, using only 2 liters of liquid He per day. This small amount of usage is due to full usage of enthalpy of boil off He going through the cassette and cooling all the components in the thin wall stainless steel 304 tubing. The details of the arrangement in the cassette are shown in Figure 6 (8).

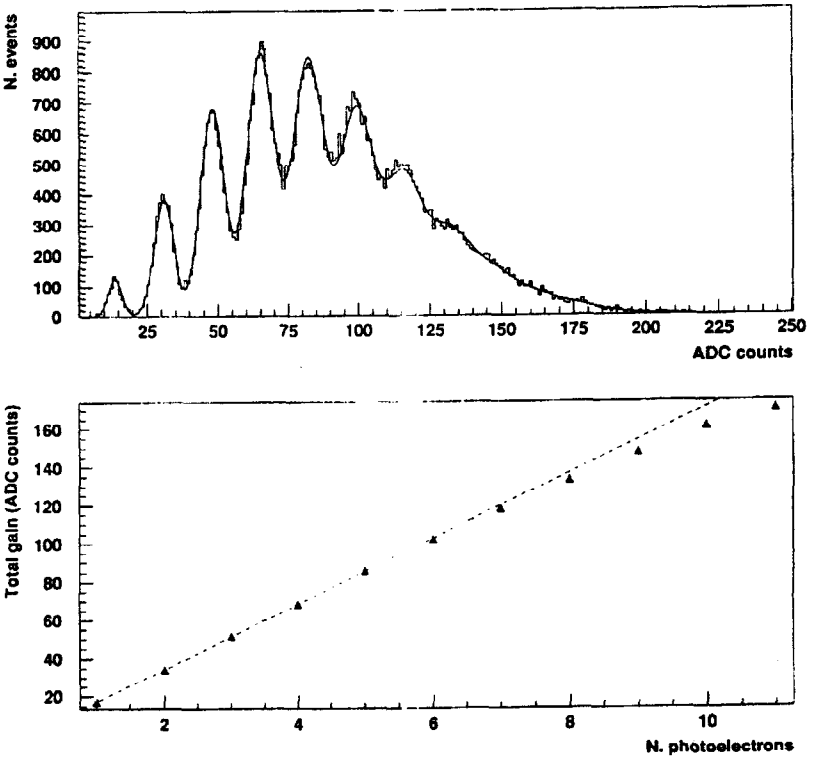

FIGURE 7. Multi-photoelectron peaks and a calibration plot. As we see in the figure, multi-photon peaks are well resolved. For this reason we call the devices "Visible Light Photon Counters" (VLPC).

SCINTILLATING FIBER TRACKING TESTS

Some scintillating fiber tracking tests were carried out using 500 micron overall diameter multiclad scintillating fibers (manufactured by Kuraray Co., Japan) and the above described cassette and cryogenic arrangement. We detected 6 photoelectrons per minimum ionizing track in the average from the middle of 280cm length of scintillating fibers (were mirrored at the end) which were coupled to 500cm length of multiclad clear optical fibers (6). An ADC counts versus number of photoelectron (pe) calibration was done before every measurement as shown in Figure 7. For this an LED was used, illuminating the optical fibers in the cassette. As seen in the figure, after the sixth photoelectron peak a small saturation appears. This is due to the amplifier saturation. The calibration was obtained by making a cut at N>2 and fitting to a convolution of Poisson and Gaussian functions:

$$f(x) = N\sum_n \frac{1}{\sigma_n\sqrt{2\pi}} exp\left[-\frac{1}{2}\left(\frac{x-n}{\sigma_n}\right)^2\right]\frac{exp(-n_{pe})}{n!} \qquad (1)$$

where the free parameters were normalization factor (N) and the mean value of the Poisson distribution (n_{pe}). Sigma of each gaussian (σ_n) was fixed by determining the peaks with the LED runs for the bias voltage and temperature.

$$\sigma_n^2 = \sigma_0^2 + \sigma_c^2 \cdot n, \tag{2}$$

where σ_c is a sigma of the n-th peak and σ_0 is a sigma value of the pedestal.

Attenuation of photons in various scintillating fibers are shown in Figure 8. The results indicate that attenuation lengths are between four and five meters and there was no appreciable change in this number for fibers of 500 microns to 1mm. Attenuation length, λ, of photons from 3HF (1500 ppm 3-Hydroxyflavone +1% P-therphenyl) scintillating fiber were measured through various diameters of multiclad clear optical fibers. The 3HF emits photons around the peak wavelength of 530nm (manufactured by Kuraray Co.). The results, as seen in the figure, indicated that the attenuation lengths of photons from the 3HF within the experimental error does not depend on fiber diameter between 0.5mm to 1mm.

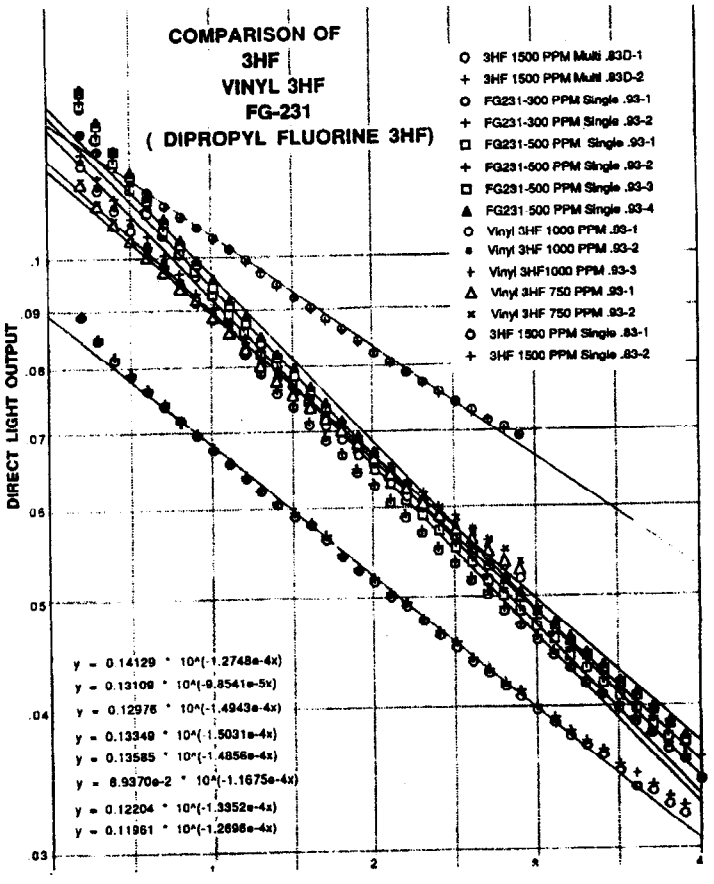

FIGURE 8. Attenuation length plots for various scintillators. There is about 80% more yield from the multi-clad fibers relative to single clad.

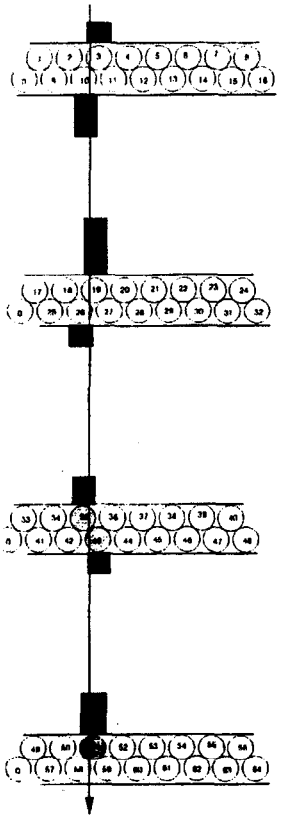

FIGURE 9. A minimizing ionizing track. The number of detected photons is indicated in the bars.

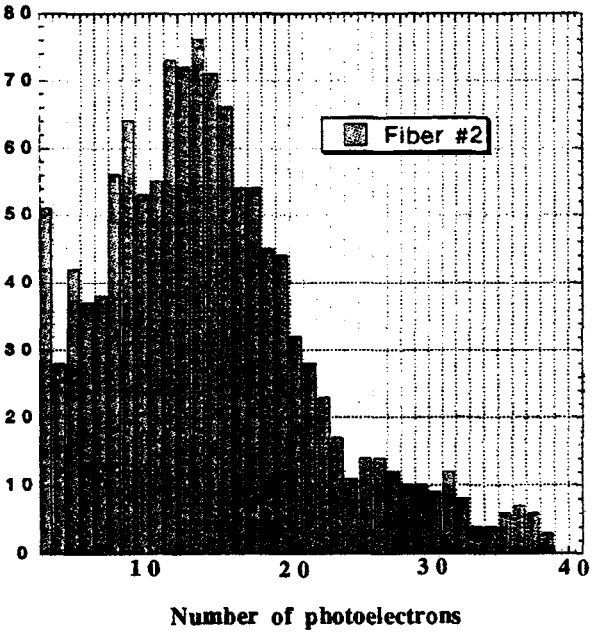

FIGURE 10. Pulse height distribution from VLPC fiber #2 when fiber is illuminated by minimum ionization particles (MIP).

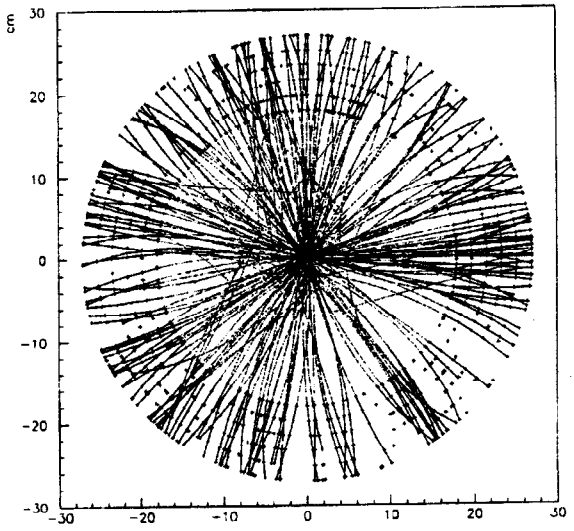

FIGURE 11A. A typical top + 6 MB event in the R-ϕ view. Crosses are axial hits, solid lines connect hits used, and dotted curves are extrapolation inward of the final parameters.

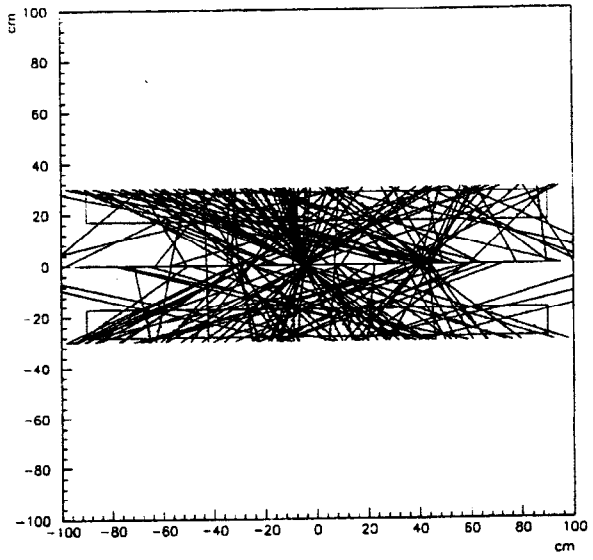

FIGURE 11B. R-Z view of a top + 6 MB event. Crosses show locations of associated stereo-hit/axial-segment points. Lines show extrapolation of fitted segment to beam line.

Some beam tests were carried out at the Meson 6 West test beam using 835 micron (scintillating core of 725 micron) multiclad 3HF fibers using author's designed cassettes (9). Four staggered doublets were used with the tests. Figure 9 shows a 15GeV hadron (most likely a pion) track with the number of photoelectrons indicated in the pulse height histograms. Figure 10 shows the number of photoelectron distribution for a fiber. Weighted average photoelectrons is more than 15. For a staggered doublet the tracking efficiency is better than 99.7%.

The Collider Detector Facility at Fermilab (CDF) has considered using scintillating fiber tracker and some track reconstructions were done using top quark events. Figures 11-a and 11-b show how efficiently fiber tracker could find tracks that were found by the Central Tracker (CTC). Presently Fermilab physicists and engineers are working hard on a large system design for the D0, Short Baseline Neutrino Experiment (COSMOS), and CP Violation Experiment at the Main Injector (KAMI). The number of VLPCs to be needed will be around 240,000.

USE OF VLPCS FOR MEDICAL APPLICATIONS

Single Fiber Tracker for Stereotactic Biopsy and Intraoperative Lumpectomy of Breast Cancer

Breast cancer in women of child bearing age is the second leading cause of death in the USA (10). Early detection has allowed for less extensive surgical procedures and/or decreased need for chemotherapy since a substantial majority of questionable lesions detected by mammography are benign. There is a growing interest among the health care professionals and patients in finding alternatives to surgical biopsy for diagnosing these lesions. State-of-the-art stereotactic breast biopsy is comparable in sensitivity to surgical biopsy, and the procedure is quicker, cheaper, and easier than the standard practice of preoperative, mammographically guided localization followed by surgical biopsy.

The problems mentioned above can be ameliorated by a nuclear medicine procedure using a beta detector on the end of a 0.8mm diameter scintillator and fiber optic cable (11). By positioning the detector within a few millimeters of the suspected area, small lesions, usually not detectable using gamma radiation detectors, can be identified and quantified for activity. The fiber optic cable with a small scintillating plastic fiber attached (fused) to the tip can either be inserted into a core biopsy, or can be used during ductogram to identify the duct system containing microcalcifiedclusters. When inserted into a surgical wand, it could be used to ensure that all residual tumor was removed during lumpectomy. This diagnostics alone is very much needed to prevent recurrence and spread of malignant tissues.

We have developed a prototype suitable probe that uses a rather small diameter biopsy needle (in the current study an 18 gauge needle with an external diameter of 1.25mm) containing a 0.83mm diameter and 3mm length 3HF (above mentioned) multiclad scintillating fiber, which is fused to the same diameter multiclad clear optical fiber of 200cm length.

Photons emitted from the scintillating fiber by the passage of betas or positrons are transmitted through the optical fiber and are detected by a VLPC. For the set up, a cassette and the cryogenics mentioned in the tracking section above were used. The

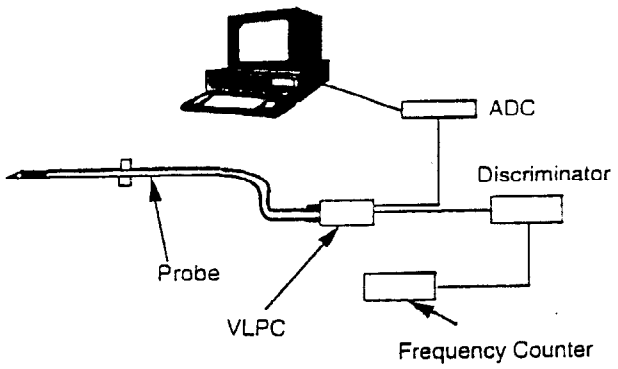

FIGURE 12. A schematic view of the biopsy needle probe together with a simple data acquisition system.

probe assembly and the rather inexpensive data acquisition system are shown in Figure 12.

The signals from the VLPC were amplified by a transimpedance amplifier (TIA), fed into a discriminator and counted by a commercial scaler. The VLPC produces an avalanche gain around 30,000 per photoelectron. We obtained less than two pulses per minute as background counts when the threshold was set above three photoelectrons. We measured experimentally that the average number of photoelectrons produced in the VLPC was more than 40, by the passage of betas through the thin scintillator. Pulse height spectrum obtained using a Bi^{207} beta source is shown in Figure 13. Only a small fraction of the 1MeV beta particle energy is left in the thin scintillator, giving rise to the pulse height spectrum.

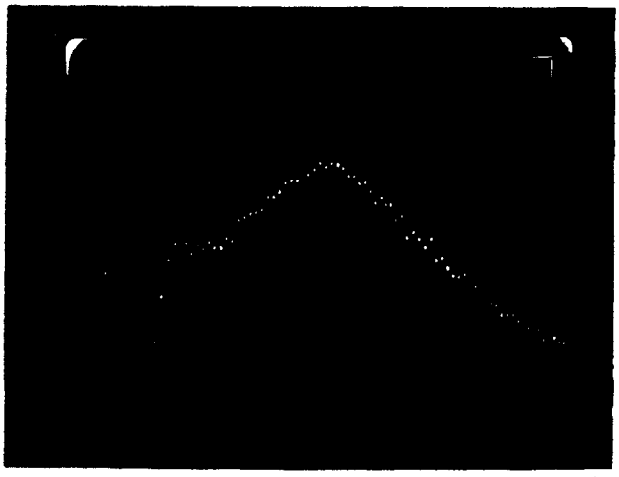

FIGURE 13. Pulse height spectrum obtained using Bi^{207} beta source. The average energy released in the scintillator fiber is about 60KeV. The peak value corresponds to 40 photoelectrons detected by the VLPC.

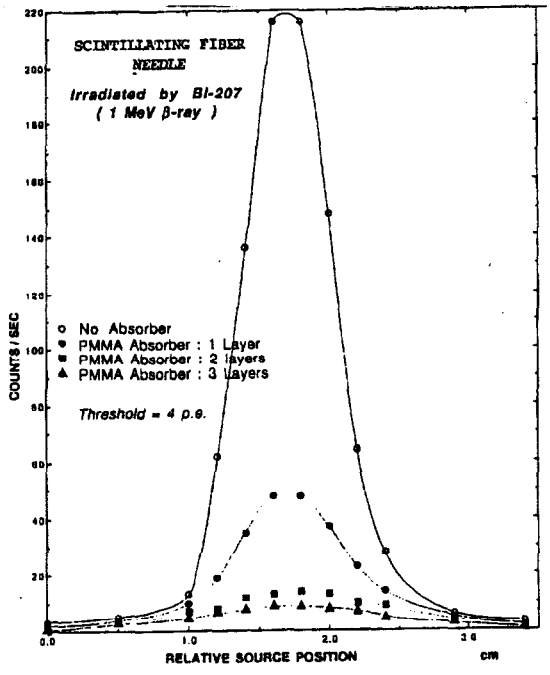

FIGURE 14. Results from the Bi^{207} source test. The curves clearly indicate that the 1MeV betas are rapidly absorbed by the 1.5mm thick Lucite sheets, and there are not many counts from gamma conversions in the scintillator although 90% of the decays from the source are gamma rays in this case.

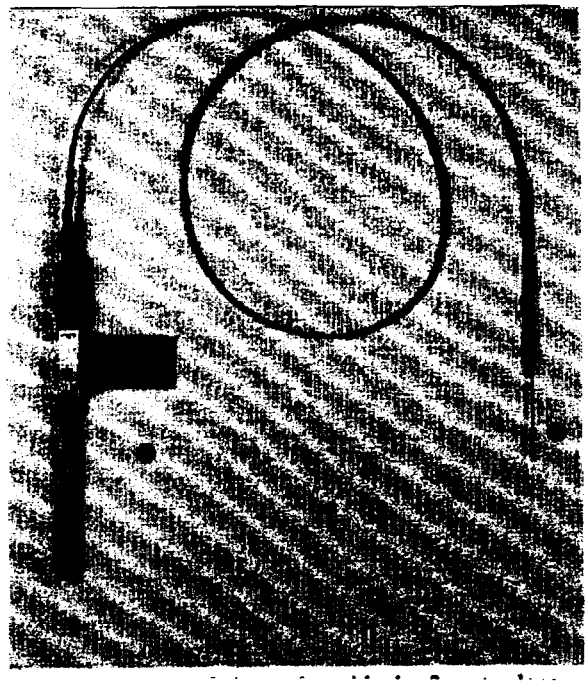

FIGURE 15. Photograph of the probe with the 2 meter long optical fiber between the biopsy needle and the VLPC unit.

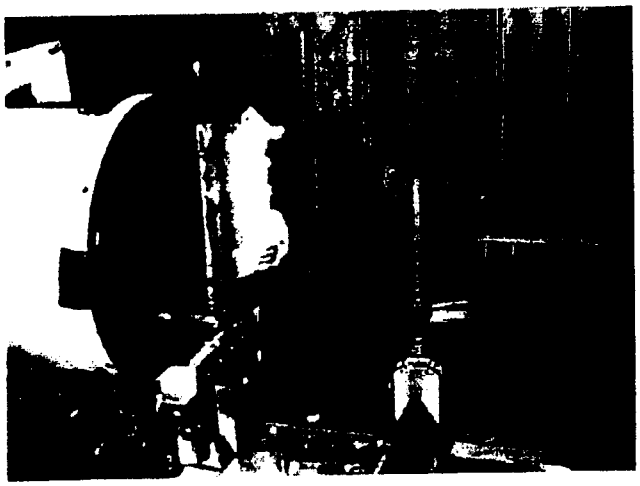

FIGURE 16. Test done with a rat having an R3230 AC in the hind leg. The rat was administered 432 microcurie FDG i.v.

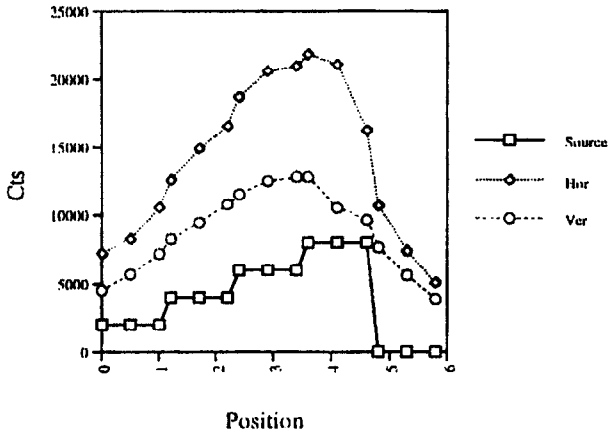

FIGURE 17. Two dimensional scan, even from outside of the skin, indicates where the radionucleide concentration is.

EXPERIMENTAL RESULTS

In order to determine point spread function, we moved the probe linearly relative to 1 microcurie Bi^{207} source without and with 1.5mm thick Lucite sheets (mimicking tissue equivalent density) in between the source and the probe, and recorded the counts per second. The source diameter was approximately 4mm and it was not collimated. The results plotted, in Figure 14 show that the 1MeV betas from the source were very much attenuated after one sheet of Lucite, but we can find the source position after 4.5mm thickness. We expect that the intrinsic resolution of the probe be better than 1mm. The curves also show that the probe is sensitive to betas and not to

gammas, although only 8% of the decays produce betas and the rest being the gamma activity. This feature is important due to the fact that the probe will not be sensitive to 511KeV gammas from positron annihilation when a positron source is traced. For a probe like this in a clinical condition, the cryogenic part can be cooled by liquid Helium vapor for safety. A photograph of the probe is shown in Figure 15.
As a first experiment, a preliminary test was done using a rat bearing R3230 adenocarcinoma. The experimental arrangement is shown in Figure 16. As shown in Figure 17, the biopsy needle was moved in an x,y matrix points and the counts were recorded. Even from outside of the skin the probe indicates where the radionucleide concentration is.

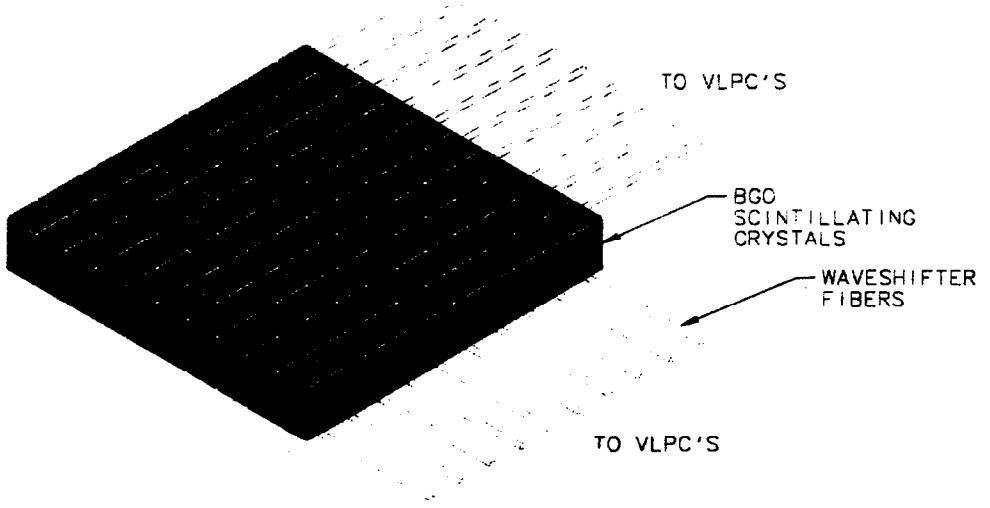

FIGURE 18. The principal scheme for detecting gamma rays in a two dimensional readout. More layers can be added depending on the energy of the gammas to be detected

USE OF VLPCS FOR PARTICLE ASTROPHYSICS

A possible way of using VLPCs as photodetectors for detecting relatively low energy gammas is shown in Figure 18. In this case wavelength shifting fibers are attached to a matrix array of scintillating crystals in an x,y arrays. The crystal size can be sufficiently large to detect multi MeV gammas from outer space. Scintillating crystals like BGO can be used in this case. Rubrene doped polystyrene can be used as wavelength shifter. Optical fiber that is coupled to wavelength shifter carries the photons to the VLPCs. This idea was proposed for medical imaging by M. Petroff, but it did not work so well due to low energy gammas, 511KeV, from positron annihilation. I am convinced that it will work here due to the detection of multi MeV gammas.

REFERENCES

1. Petroff, M.D. and Atac, M. , *IEEE Trans. on Nucl. Sci.* NS-36 (1989) 163.
2. Atac, M., Park, J., Cline, D., Chrisman, D., Petroff, M. and Anderson;E., Nucl. Instr. and Meth. A314 (1992) 56.
3. Atac, M., et al.; *Nucl. Instr .and Meth.* A320 (1992) 155.
4. Alitti, J., et al.; *Nucl. Instr. and Meth.* A279 (1989) 364.
5. Petroff, M.D., Stapelbroek, M.G., and Kleinhans, W.A., *Appl. Phys. Lett.* Vol.51 No.6 (1987) 406.
6. Atac, M., Mishina, M., Takano, T., Valls, J., Yasuokka, K. and Yoshida, T., CDF/ANAL/Tracking/Public/3569, April 11, 1996.
7. Zimmerman, T., *IEEE Trans. Nuc. Sci.* NS-37(2), (1992) 439.
8. Gubinelli, M., Tonet, O.,. Sorel, M., Atac, M., Mishina, M., and Valls; J., CDF/Pub/ Public/4154, July, 1997.
9. Atac, M., Cline, D., Pischalnikov, Y., and Rhoades, J.; Presented at the SciFi Conference at Notre Dame.
10. Titcomb, C.L., *Hawaii Medical Journal*, Vol. 49 (1990) 18.
11. Atac, M., Nalcioglu, O., and Roeck, W., unpublished report.